THE EUROPEAN
PHYSICAL JOURNAL C

Higgs boson production at the LHC: fast and precise predictions in QCD at higher orders

Stefano Camarda[1], Leandro Cieri[2], Giancarlo Ferrera[3,a], Jesús Urtasun-Elizari[3]

[1] CERN, 1211 Geneva, Switzerland
[2] Instituto de Física Corpuscular, Universitat de València-CSIC, Parc Científic, 46980 Paterna, Valencia, Spain
[3] Dipartimento di Fisica, Università di Milano and INFN, Sezione di Milano, 20133 Milan, Italy

Abstract We present a new numerical program, `HTurbo`, which provides fast and numerically precise predictions for Higgs boson production cross sections. The present version of the code implements the perturbative QCD expansion up to the next-to-next-to-leading order also combined with the resummation of the large logarithmic corrections at small transverse momenta up to next-to-next-to-leading logarithmic accuracy and it includes the Higgs boson production through gluon fusion and decay in two photons with the full dependence on the final-state kinematics. Arbitrary kinematical cuts can be applied to the final states in order to obtain fiducial cross sections and associated kinematical distributions. We present a benchmark comparison with the predictions obtained with the numerical programs `HRes` and `HNNLO` programs for which `HTurbo` represents an improved reimplementation.

After the discovery of the Higgs boson [1,2], a foremost goal of the physics program at the Large Hadron Collider (LHC) has become the direct investigation of the electroweak symmetry breaking mechanism. In particular, precision studies are a key tool for searches of possible deviations from Standard Model (SM) predictions in the Higgs sector.

In this paper we consider the production of the SM Higgs boson through gluon fusion and its decay to $\gamma\gamma$. The gluon fusion subprocess $gg \rightarrow H$ [3], through a heavy-quark (mainly, top-quark) loop, is the main production mechanism of the SM Higgs boson at hadron colliders and its dynamics is driven by strong interactions. Therefore, it is essential to study the effects of higher-order QCD radiative corrections and to provide accurate theoretical predictions of Higgs boson cross sections and associated distributions.

The QCD radiative corrections to the total cross sections and differential distributions have been calculated up to next-to-next-to-next-to-leading order (N^{3}LO) within the framework of the large-M_{top} approximation [4–17]. The NNLO parton-level calculation of H+jet production has been performed in Refs. [18–20]. The combination of the QCD transverse-momentum (q_T) resummation formalism of logarithmically enhanced contribution with fixed-order perturbative results at different levels of theoretical accuracy, have been obtained in [16,21–26] (see also references therein).

Theoretical predictions depend on several different parameters and on various inputs such as parton density functions (PDFs), renormalization and factorization scales and SM parameters. In order to obtain precise theoretical predictions with a reliable estimate of the associated uncertainties it is therefore crucial to develop computing codes which allow for fast calculations with small numerical uncertainties.

The `HTurbo` program, which is presented in this paper, provides fast and numerically precise predictions of the Higgs boson production and decay cross sections. It follows the structure of the `DYTurbo` code [27] developed for Drell–Yan lepton pair production. Performance enhancements are primarily achieved through the use of numerical integrations with quadrature rules based on interpolating functions, software profiling optimization and multi-threading implementation.

`HTurbo` calculates higher-order QCD corrections of Higgs boson cross sections at fully differential level in the four momenta of the final states by implementing the q_T resummation formalism developed in Refs. [28–31] and the q_T subtraction method of Ref. [11] in a completely independent way from the original numerical programs `HqT` [29,32], `HNNLO` [11] and `HRes` [23]. Besides an improvement in performances and numerical precision, this novel implementation has the aim of facilitating the inclusion of N^{3}LO corrections along the lines of Ref. [33] and the fiducial perturbative power corrections within the q_T subtraction method

Springer

exploiting the recoil procedure of Ref. [34] as performed in Ref. [35].[1]

The present version of the program includes the Higgs boson production through gluon fusion and its decay in a photon pair, implementing the resummation of the QCD contributions logarithmically-enhanced in the small-q_T region at leading-logarithmic (LL), next-to-leading-logarithmic (NLL), and NNLL accuracy as well as the corresponding finite-order contributions at next-to-leading order (NLO) and NNLO both in the small- and large-q_T regions.[2] The fully-differential fixed-order QCD calculation has been implemented up to next-to-next-to-leading order (NNLO). The H+jet predictions have been reimplemented from the MCFM program [36,37], as encoded in HRes and HNNLO. The HTurbo program is based on a modular C++ structure (with few Fortran functions interfaced) with multi-threading implemented with OpenMP and through the Cuba library [38]. The parameters of the calculation can be set in a flexible way via input file and/or command line options. The HTurbo program will be made publicly available.

We briefly summarize the relevant formulae which have been implemented in the HTurbo program.[3] The fully-differential Higgs boson cross section, completely inclusive over the final-state QCD radiation, is described by six kinematic variables corresponding to the momenta of the two photons. Therefore we can express the cross-section as a function of the transverse momentum q_T, the rapidity y and the invariant mass m of the Higgs boson (or photon pair), and three angular variables corresponding to the polar θ and the azimuthal ϕ angles of the photon decay in a given Higgs boson rest frame and to the azimuth ϕ_H of the Higgs boson in the laboratory frame. Given the spin-0 nature of the SM Higgs boson the cross section factorizes in two independent factors for the Higgs boson production and decay subprocesses. We treat the Higgs boson within the narrow-width approximation, $\Gamma_H/m_H \to 0$ (Γ_H is the Higgs boson total decay width), and thus we have $m = m_H$. Moreover in (unpolarised) hadron collisions the initial-state hadrons, i.e. the incoming beams, are to very good approximation azimuthally symmetric and therefore the cross section does not depend on the absolute value of ϕ_H. Therefore in the following we will consider the cross section averaged over ϕ_H at fixed values of the additional kinematical variables of the final-state system.

The q_T resummed cross section can be written as

$$d\sigma_{N^nLL+N^nLO}^{H} = d\sigma_{N^nLL}^{res} - d\sigma_{N^{n-1}LO}^{asy} + d\sigma_{N^{n-1}LO}^{f.o.}, \qquad (1)$$

with $n = 1, 2, 3, \ldots$ (in the following we do not explicitly consider the lowest order predictions at LL accuracy: $d\sigma_{LL}^{H} = d\sigma_{LL}^{res}$). The term $d\sigma^{res}$ in Eq. (1) is the resummed component, $d\sigma^{asy}$ is the asymptotic contribution (that is the fixed-order expansion of $d\sigma^{res}$), and $d\sigma^{f.o.}$ is the finite-order cross section integrated over final-state QCD radiation (which can be obtained from the H+jet cross section). The resummed term $d\sigma^{res}$ dominates at small q_T ($q_T \ll m$) while the finite-order component $d\sigma^{f.o.}$ describes the large-q_T region ($q_T \sim m$). An accurate description of the region of intermediate q_T requires a consistent match between the resummed and finite components.

The resummation of the logarithmic contributions has been carried out in the impact-parameter space b (which is the Fourier-conjugate variable to q_T) [39] in order to fulfill the constraint of transverse-momentum conservation for multi-parton radiation. Moreover convolution with PDFs is more conveniently expressed by considering double Mellin moments of the corresponding partonic functions [30]. The resummed and asymptotic terms in Eq. (1) can thus be written as:[4]

$$d\sigma_{N^nLL}^{res} = d\hat{\sigma}_{LO}^{H} \times \mathcal{H}_{N^nLO}^{H} \times \exp\{\mathcal{G}_{N^nLL}\} \qquad (2)$$

$$d\sigma_{N^{n-1}LO}^{asy} = d\hat{\sigma}_{LO}^{H} \times \Sigma^{H}(q_T/Q)_{N^{n-1}LO}, \qquad (3)$$

where $Q \sim m$ denotes the so-called resummation scale [29], an auxiliary scale that is introduced in $d\sigma^{res}$ and, consistently, in $d\sigma^{asy}$ whose variations can be used to estimate the uncertainty from not yet calculated higher-order logarithmic corrections. The factor $d\hat{\sigma}_{LO}^{H}$ is the Born level cross section, the coefficient $\mathcal{H}^H$ [40] is the (process dependent) hard-collinear function and the term $\exp(\mathcal{G})$ is the gluon Sudakov form factor [41–43] which resums in an exponential form the large logarithmic corrections in the impact-parameter space b. The function $\Sigma^H(q_T/Q)$, which embodies the singular behaviour of $d\sigma^{f.o.}$ in the limit $q_T \to 0$, can be obtained from the fixed-order expansion of the term $\mathcal{H}^H \times \exp\{\mathcal{G}\}$.

The Mellin moments of the hard-collinear function $\mathcal{H}^H$ have been computed with the FORM [44] packages summer [45] and harmpol [46], using the method of Ref. [47]. The Mellin space evolution of PDFs and the Mellin moments of the splitting functions have been calculated with the package QCD-PEGASUS [48].

The HTurbo program includes also fixed-order predictions (without the resummation of logarithmically-enhanced contributions). Beyond the LO, the fixed-order cross section

---

[1] We note however that in order to reach this goal a necessary ingredient is the NNLO QCD prediction for H+jet production [18–20] which, at present, is not available in a public form.

[2] Sometimes in the literature this is referred respectively as NLL′ and NNLL′ accuracy.

[3] The reader interested on the details of the q_T resummation and q_T subtraction formalisms is referred to the original literature [11,28–31].

[4] For the sake of simplicity we use a symbolic notation where convolution with PDFs, the sum over different initial-state partonic channels and the inverse Mellin and Fourier transformations are understood.

is computed through the q_T subtraction formalism [11] and is expressed as the sum of three terms as follows:

$$d\sigma^H_{N^nLO} = \mathcal{H}^H_{N^nLO} \times d\sigma^H_{LO} + \left[d\sigma^{H+jet}_{N^{n-1}LO} - d\sigma^{CT}_{N^{n-1}LO} \right], \quad (4)$$

where the term $d\sigma^{H+jet}$ is the H+jet cross section, and the counter-term $d\sigma^{CT}_{N^{n-1}LO}$ is given by

$$d\sigma^{CT}_{N^{n-1}LO} = d\sigma^H_{LO} \times \int_0^\infty d^2q'_T \, \Sigma^H(q'_T/m)_{N^{n-1}LO}. \quad (5)$$

The singular behaviour of $d\sigma^{H+jet}$ in the limit $q_T \to 0$, known from the q_T resummation formalism, is the same of the subtraction counter-term $d\sigma^{CT}$. Being the terms $d\sigma^{H+jet}$ and $d\sigma^{CT}$ in Eq. (4) separately divergent at $q_T = 0$ a technical parameter $q_T^{cut} > 0$ has to be introduced. For $q_T \geq q_{T_{cut}}$ the sum of the terms in the square bracket of Eq. (4) is infrared finite (or, more precisely, integrable over q_T) and the "exact" value of the cross section can be obtained evaluating the square bracket term in Eq. (4) in the limit $q_{T_{cut}} \to 0$. However for finite value of q_T^{cut} the cross section in Eq. (4) contains perturbative power corrections ambiguities $\mathcal{O}((q_T^{cut}/M)^p)$ [49–52], with $p > 0$ which are particularly severe in the case of fiducial selection cuts which yield an acceptance that has a residual linear dependence on q_T^{cut} [50,53,54]. A method to remove such linear fiducial power corrections (FPC) within the q_T subtraction formalism has been proposed in Refs. [35,55].

An important feature of the resummation formalism of Ref. [29] is the so called unitarity constraint which leads to the following relation:

$$\int_0^\infty dq_T^2 \, d\sigma^{res}_{N^nLL+N^nLO} = \mathcal{H}^H_{N^nLO} \times d\hat{\sigma}^H_{LO}, \quad (6)$$

which ensures that fixed-order results are exactly recovered upon integration over q_T of the matched cross section. A consequence of the unitarity constraint is the reduction of resummation effects in the region of small impact parameter where it is clear that resummation cannot give an improvement over the accuracy of the fixed-order calculation. The effect of unjustified resummed contributions in the large-q_T region can be further reduced or eliminated by introducing a switching function $w(q_T, m)$ which multiplies the terms $d\sigma^{res}_{N^nLL}$ and $d\sigma^{asy}_{N^{n-1}LO}$ in Eq. (1) above a given q_T value. However because such switching violates the unitarity constraint of Eq. (6) it has to be included with some care. Within HTurbo the effect of a Gaussian switching function $w(q_T, m)$ chosen following Ref. [34] can be included.

The perturbative form factor $\exp(\mathcal{G})$ is formally singular when transverse-momenta of the order of the scale of the Landau pole of the QCD coupling ($b^{-1} \sim \Lambda_{QCD}$) are approached. This is the indication of the breakdown of perturbation theory and of the onset of truly non-perturbative (NP) effects. In this region a model for NP QCD effects, which

has to include a regularization of the Landau singularity, is necessary. We have explicitly implemented in the HTurbo program the so-called *Minimal Prescription* [56–58] which regularizes the Landau singularity in resummed calculations without introducing higher-twist power-suppressed contributions of the type $\mathcal{O}(\Lambda_{QCD}/Q)$. Alternatively it can be chosen the freezing procedure [59,60] known as the 'b_* prescription', which is implemented in HRes, consisting in the replacement

$$b^2 \to b_*^2 = b^2 \, b_{\lim}^2/(b^2 + b_{\lim}^2) \quad (7)$$

in the form factor $\exp(\mathcal{G})$. The value of the parameter $b_{\lim}$ has to be set to be slightly smaller than the Landau singularity $b^{-1} \sim \Lambda_{QCD}$. Power-suppressed contributions are expected to dominate at very small transverse-momentum ($q_T \sim \Lambda_{QCD}$) and to correctly describe the experimental data in that region they have to be (properly) included taking into account the delicate interplay with the leading-twist term. We parameterize the NP QCD effects at low q_T through a non-perturbative form factor with different functional forms (the simplest one is a Gaussian smearing factor, $\exp(-g_{NP}b^2)$, which depends on the non perturbative parameter g_{NP}).

In the following we show some benchmark numerical results obtained with HTurbo compared with corresponding results from HRes (up to NNLL+NNLO accuracy) and HNNLO (up to NNLO). In particular we consider the cross section differential in the Higgs boson q_T in both the full final state diphoton phase space and in a given selected fiducial region. We also compare the time performance of the codes in order to assess the performance improvement of HTurbo.

We consider Higgs boson cross sections in proton–proton collisions at $\sqrt{s} = 13$ TeV using the NNPDF3.1 NNLO [61] set of parton density functions with $\alpha_S(m_Z) = 0.118$. The computation is performed by considering $gg \to H$ production, through a top-quark loop, in the large-M_{top} approximation. We use the same settings and input parameters in both the HTurbo and HRes codes. In particular the value of the renormalization (μ_R), factorization (μ_F) and resummation (Q) scales have been chosen to be equal to the Higgs boson mass m_H. We start to present our benchmark results at inclusive level (i.e. integrating over the diphoton final state kinematics). In Fig. 1 we consider the resummed part of the q_T distribution (see Eq. (2)) at NLL accuracy (left panel) and at NNLL accuracy (right panel). The HTurbo results using quadrature integration (blue dots) have been compared with the HRes results (green histograms). The lower panels show the ratio between the results which are in agreement, within the numerical uncertainties of the codes, at better than 1% level. In Fig. 2 we consider the asymptotic term of the cross section (see Eq. (2)) at LO (left panel) and NLO (right panel). The asymptotic term diverges in the $q_T \to 0$ limit and it becomes negative at large q_T (we thus show the abso-
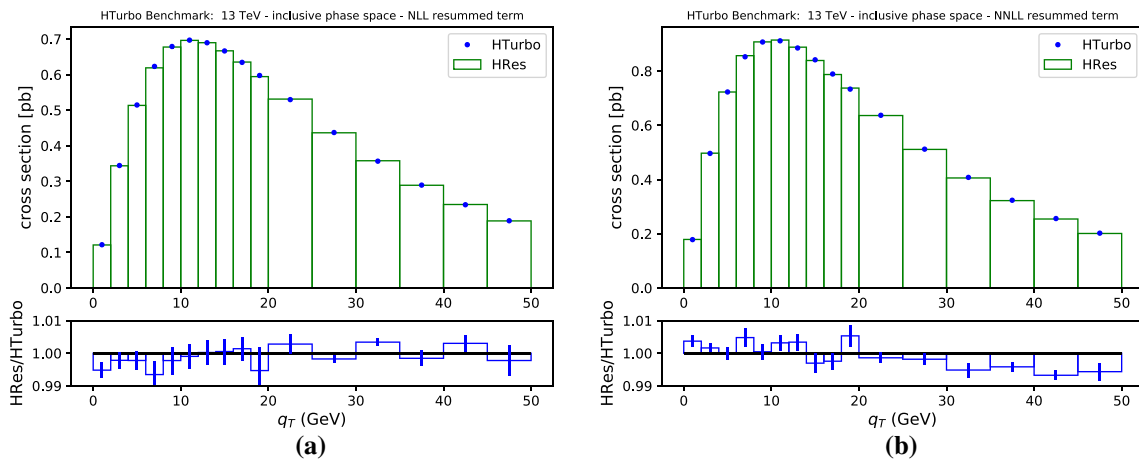
Fig. 1 Comparison of full-photon phase space differential cross sections computed with HRes and HTurbo at $\sqrt{s} = 13$ TeV. Resummed component of the transverse momentum distribution at NLL (**a**) and NNLL (**b**) accuracy. The top panels show absolute cross sections, and the bottom panels show ratios of HTurbo to HRes results
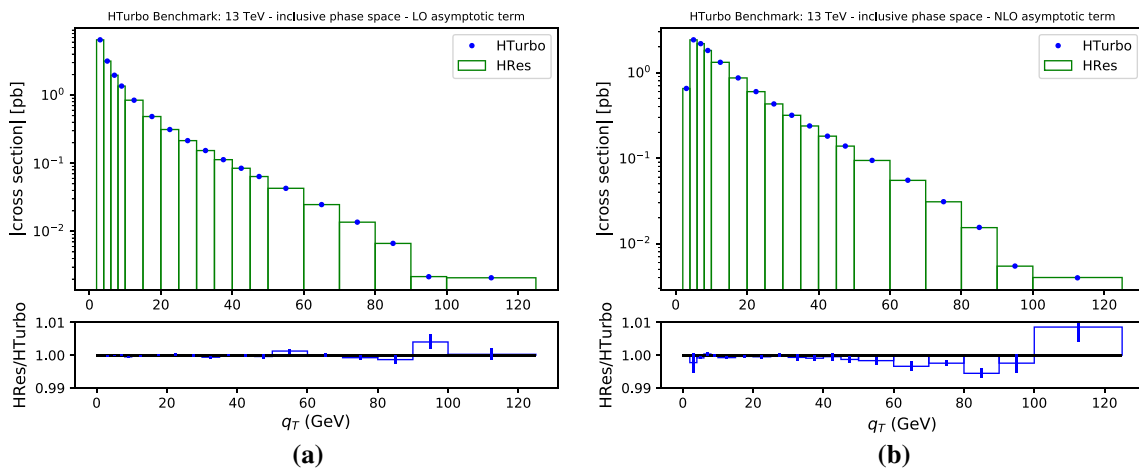

Fig. 2 Comparison of full-photon phase space differential cross sections computed with HRes and HTurbo at $\sqrt{s} = 13$ TeV. Absolute value of the asymptotic component of the transverse momentum distribution at LO (**a**) and NLO (**b**) accuracy. The top panels show absolute cross sections, and the bottom panels show ratios of HTurbo to HRes results

lute value of the results in logarithmic scale). The q_T distribution of the asymptotic term has been computed in the range $1\,\text{GeV} < q_T < m_H$ and we obtained a sub-percent agreement between HTurbo (blue dots) using quadrature integration and HRes (green histograms) results. Finally, in Fig. 3, we show the fixed-order term of the cross section at LO (left panel) and NLO (right panel) as obtained with HTurbo and HNNLO. As both HTurbo and HNNLO programs use the Vegas algorithm for numerical integration, we expect to observe similar results as is confirmed by the sub-percent agreement between HTurbo (blue dots) and HNNLO (green histograms) results.

We then consider the case of fiducial cross sections. The fiducial phase space is defined by the photon transverse momenta $p_T^\gamma > 0.35\,m_H$ and the photon pseudorapidities $|\eta^\gamma| < 2.37$. In Figs. 4, 5 and 6 we show the comparison between the resummed, asymptotic and fixed-order term as presented above for the inclusive phase space. Also in the case of fiducial phase space we observe a sub-percent agreement between HTurbo (blue dots), HRes and HNNLO (green histograms) results in the entire range of q_T considered.

We now briefly comment on various tests of time performance which have been performed on a machine with 3.50 GHz Intel Xeon CPUs. The computation time necessary to calculate cross-section predictions for HTurbo and HRes is compared and used to assess the performance improvement of HTurbo. The HRes calculation for the resummed term of the inclusive cross-section at NLL accuracy with an uncertainty of 1% took around 0.5 h, while the analogous HTurbo calculation (without the multi-threading option)
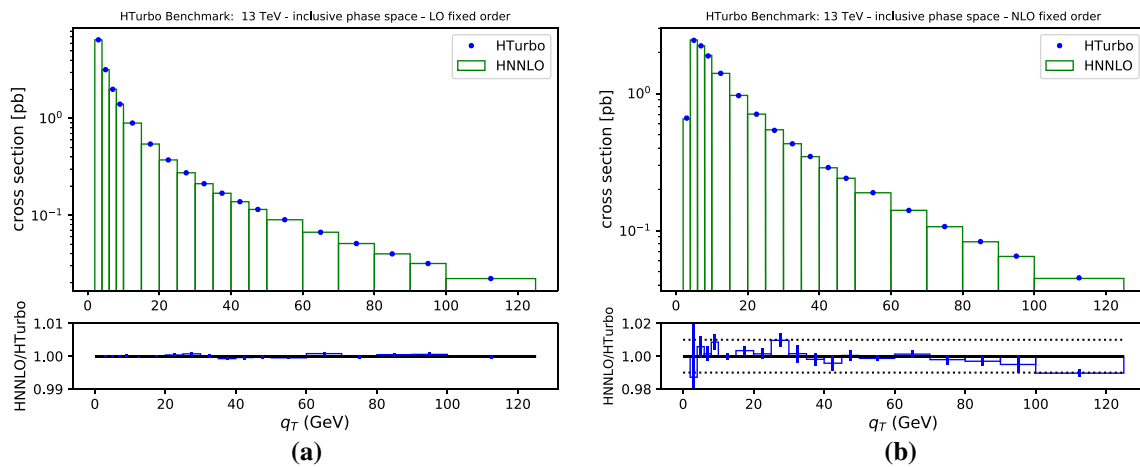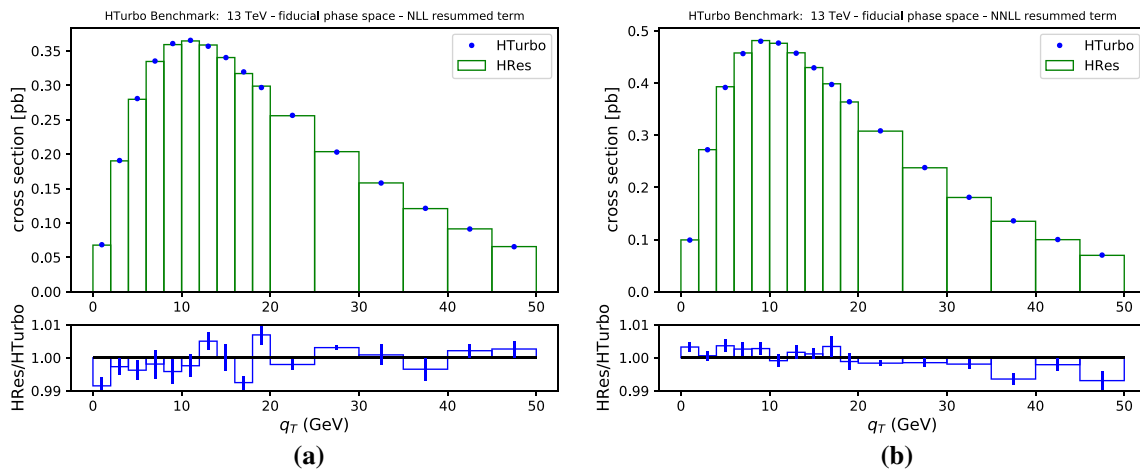
Fig. 3 Comparison of full-photon phase space differential cross sections computed with HRes and HTurbo at $\sqrt{s} = 13$ TeV. Fixed-order component of the transverse momentum distribution at LO (**a**) and NLO (**b**) accuracy. The top panels show absolute cross sections, and the bottom panels show ratios of HTurbo to HRes results

Fig. 4 Comparison of full-photon phase space differential cross sections computed with HRes and HTurbo at $\sqrt{s} = 13$ TeV. Resummed component of the transverse momentum distribution at NLL (**a**) and NNLL (**b**) accuracy. The top panels show absolute cross sections, and the bottom panels show ratios of HTurbo to HRes results

with an uncertainty of 0.001% took around 20 s, yielding an improvement of around two orders of magnitude in the time performance and three orders of magnitude in numerical precision. Similar results were obtained including fiducial cuts or considering the resummed term at NNLL accuracy. The LO or NLO calculation of the asymptotic term took around 10 minutes with an uncertainty of 0.5-1% within HRes both at inclusive level and with fiducial cuts, while the analogous HTurbo single-thread calculation with a similar accuracy took from 3 s (inclusive case) up to 30 s (fiducial case), yielding an improvement of one or two orders of magnitudes in the time performance. Finally, the fixed-order term of the cross section represents the most time-consuming part of the calculation; the computation at NLO (LO) with 1% (0.05%)

accuracy required 30 min (1 min) both within HNNLO and HTurbo single-thread. However we observe that the fixed-order part of the calculation could be computed by using fast interpolation techniques [62,63].

In conclusion, we have presented the HTurbo numerical program which provides fast and numerically precise predictions for Higgs boson production through a new implementation of the HqT, HRes and HNNLO codes, following the improvements of the DYTurbo program [27] for Drell–Yan lepton pair production. HTurbo implements the fully-differential fixed-order QCD calculation for Higgs boson production (via gluon fusion) and decay as well as the resummation of the large logarithmic corrections at small transverse momenta. The present version of the code reaches
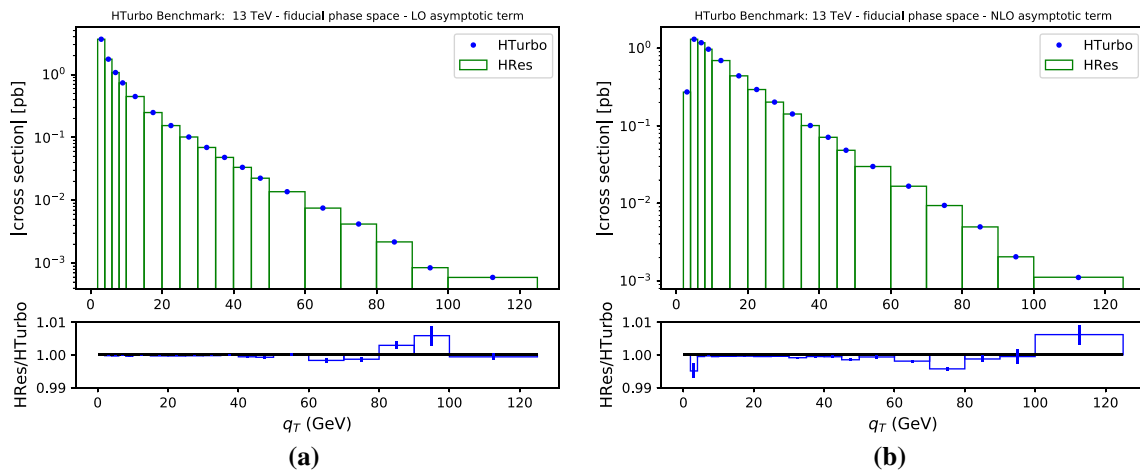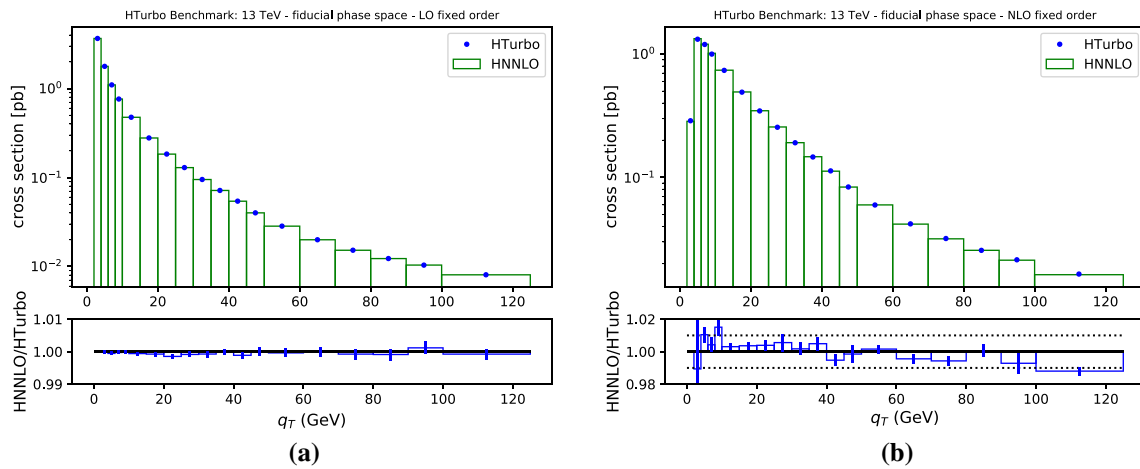
(a)

Fig. 5 Comparison of fiducial differential cross sections computed with HRes and HTurbo at $\sqrt{s} = 13$ TeV. The fiducial phase space is defined in the text. Absolute value of the asymptotic component of

the transverse momentum distribution at LO (**a**) and NLO (**b**) accuracy. The top panels show absolute cross sections, and the bottom panels show ratios of HTurbo to HRes results

(a)

Fig. 6 Comparison of fiducial differential cross sections computed with HRes and HTurbo at $\sqrt{s} = 13$ TeV. The fiducial phase space is defined in the text. Fixed-order component of the transverse momen-

tum distribution at LO (**a**) and NLO (**b**) accuracy. The top panels show absolute cross sections, and the bottom panels show ratios of HTurbo to HRes results.

the next-to-next-to-leading order and next-to-next-to-leading logarithmic accuracy, and it includes the decay of the Higgs boson into two photons. The enhancement in performance of HTurbo over the previous programs (which reaches two orders of magnitude for the resummed term) is achieved by optimizing the code, factorizing the cross section into production and decay variables, and using numerical integration quadrature rules based on interpolating functions. The resulting cross-section predictions are in agreement with the results of the original programs. The great reduction in computing time for performing cross-sections calculation opens new possibilities for Higgs boson physics and facilitates an efficient inclusion of N^{3}LO corrections along the lines of Refs. [33,35].

Data Availability Statement This manuscript has no associated data or the data will not be deposited. [Authors' comment: This is a theoretical study and has no associated experimental data.]

References

1. G. Aad et al. [ATLAS], Phys. Lett. B **716**, 1–29 (2012). https://doi.org/10.1016/j.physletb.2012.08.020. arXiv:1207.7214 [hep-ex]
2. S. Chatrchyan et al. [CMS], Phys. Lett. B **716**, 30–61 (2012). https://doi.org/10.1016/j.physletb.2012.08.021. arXiv:1207.7235 [hep-ex]
3. H.M. Georgi, S.L. Glashow, M.E. Machacek, D.V. Nanopoulos, Phys. Rev. Lett. **40**, 692 (1978). https://doi.org/10.1103/PhysRevLett.40.692
4. S. Dawson, Nucl. Phys. B **359**, 283–300 (1991). https://doi.org/10.1016/0550-3213(91)90061-2
5. A. Djouadi, M. Spira, P.M. Zerwas, Phys. Lett. B **264**, 440–446 (1991). https://doi.org/10.1016/0370-2693(91)90375-Z
6. M. Spira, A. Djouadi, D. Graudenz, P.M. Zerwas, Nucl. Phys. B **453**, 17–82 (1995). https://doi.org/10.1016/0550-3213(95)00379-7. arXiv:hep-ph/9504378 [hep-ph]
7. R.V. Harlander, W.B. Kilgore, Phys. Rev. Lett. **88**, 201801 (2002). https://doi.org/10.1103/PhysRevLett.88.201801 arXiv:hep-ph/0201206
8. C. Anastasiou, K. Melnikov, Nucl. Phys. B **646**, 220–256 (2002). https://doi.org/10.1016/S0550-3213(02)00837-4 arXiv:hep-ph/0207004
9. V. Ravindran, J. Smith, W.L. van Neerven, Nucl. Phys. B **665**, 325–366 (2003). https://doi.org/10.1016/S0550-3213(03)00457-7 arXiv:hep-ph/0302135
10. C. Anastasiou, K. Melnikov, F. Petriello, Phys. Rev. Lett. **93**, 262002 (2004). https://doi.org/10.1103/PhysRevLett.93.262002 arXiv:hep-ph/0409088
11. S. Catani, M. Grazzini, Phys. Rev. Lett. **98**, 222002 (2007). https://doi.org/10.1103/PhysRevLett.98.222002 arXiv:hep-ph/0703012
12. C. Anastasiou, C. Duhr, F. Dulat, F. Herzog, B. Mistlberger, Phys. Rev. Lett. **114**, 212001 (2015). https://doi.org/10.1103/PhysRevLett.114.212001 arXiv:1503.06056 [hep-ph]
13. B. Mistlberger, JHEP **05**, 028 (2018). https://doi.org/10.1007/JHEP05(2018)028 arXiv:1802.00833 [hep-ph]
14. F. Dulat, B. Mistlberger, A. Pelloni, Phys. Rev. D **99**(3), 034004 (2019). https://doi.org/10.1103/PhysRevD.99.034004 arXiv:1810.09462 [hep-ph]
15. L. Cieri, X. Chen, T. Gehrmann, E.W.N. Glover, A. Huss, JHEP **02**, 096 (2019). https://doi.org/10.1007/JHEP02(2019)096 arXiv:1807.11501 [hep-ph]
16. G. Billis, B. Dehnadi, M.A. Ebert, J.K.L. Michel, F.J. Tackmann, Phys. Rev. Lett. **127**(7), 072001 (2021). https://doi.org/10.1103/PhysRevLett.127.072001 arXiv:2102.08039 [hep-ph]
17. X. Chen, T. Gehrmann, E.W.N. Glover, A. Huss, B. Mistlberger, A. Pelloni, Phys. Rev. Lett. **127**(7), 072002 (2021). https://doi.org/10.1103/PhysRevLett.127.072002 arXiv:2102.07607 [hep-ph]
18. X. Chen, T. Gehrmann, E.W.N. Glover, M. Jaquier, Phys. Lett. B **740**, 147–150 (2015). https://doi.org/10.1016/j.physletb.2014.11.021 arXiv:1408.5325 [hep-ph]
19. R. Boughezal, F. Caola, K. Melnikov, F. Petriello, M. Schulze, Phys. Rev. Lett. **115**(8), 082003 (2015). https://doi.org/10.1103/PhysRevLett.115.082003 arXiv:1504.07922 [hep-ph]
20. R. Boughezal, C. Focke, W. Giele, X. Liu, F. Petriello, Phys. Lett. B **748**, 5–8 (2015). https://doi.org/10.1016/j.physletb.2015.06.055 arXiv:1505.03893 [hep-ph]
21. Y. Gao, C.S. Li, J.J. Liu, Phys. Rev. D **72**, 114020 (2005). https://doi.org/10.1103/PhysRevD.72.114020 arXiv:hep-ph/0501229
22. Q.H. Cao, C.R. Chen, Phys. Rev. D **76**, 073006 (2007). https://doi.org/10.1103/PhysRevD.76.073006 arXiv:0704.1344 [hep-ph]
23. D. de Florian, G. Ferrera, M. Grazzini, D. Tommasini, JHEP **06**, 132 (2012). https://doi.org/10.1007/JHEP06(2012)132 arXiv:1203.6321 [hep-ph]
24. T.R. Rabemananjara, JHEP **12**, 073 (2020). https://doi.org/10.1007/JHEP12(2020)073 arXiv:2007.09164 [hep-ph]
25. T. Becher, T. Neumann, JHEP **03**, 199 (2021). https://doi.org/10.1007/JHEP03(2021)199 arXiv:2009.11437 [hep-ph]
26. E. Re, L. Rottoli, P. Torrielli, https://doi.org/10.1007/JHEP09(2021)108. arXiv:2104.07509 [hep-ph]
27. G. Bozzi, S. Catani, G. Ferrera, D. de Florian, M. Grazzini, Phys. Lett. B **696**, 207–213 (2011). https://doi.org/10.1016/j.physletb.2010.12.024 arXiv:1007.2351 [hep-ph]
28. S. Catani, D. de Florian, M. Grazzini, Nucl. Phys. B **596**, 299–312 (2001). https://doi.org/10.1016/S0550-3213(00)00617-9 arXiv:hep-ph/0008184
29. G. Bozzi, S. Catani, D. de Florian, M. Grazzini, Nucl. Phys. B **737**, 73–120 (2006). https://doi.org/10.1016/j.nuclphysb.2005.12.022 arXiv:hep-ph/0508068
30. G. Bozzi, S. Catani, D. de Florian, M. Grazzini, Nucl. Phys. B **791**, 1–19 (2008). https://doi.org/10.1016/j.nuclphysb.2007.09.034 arXiv:0705.3887 [hep-ph]
31. S. Catani, M. Grazzini, Nucl. Phys. B **845**, 297–323 (2011). https://doi.org/10.1016/j.nuclphysb.2010.12.007 arXiv:1011.3918 [hep-ph]
32. D. de Florian, G. Ferrera, M. Grazzini, D. Tommasini, JHEP **11**, 064 (2011). https://doi.org/10.1007/JHEP11(2011)064 arXiv:1109.2109 [hep-ph]
33. S. Camarda, L. Cieri, G. Ferrera, Phys. Rev. D **104**, L111503 (2021). https://doi.org/10.1103/PhysRevD.104.L111503 arXiv:2103.04974 [hep-ph]
34. S. Catani, D. de Florian, G. Ferrera, M. Grazzini, JHEP **12**, 047 (2015). https://doi.org/10.1007/JHEP12(2015)047 arXiv:1507.06937 [hep-ph]
35. S. Camarda, L. Cieri, G. Ferrera, arXiv:2111.14509 [hep-ph]
36. J.M. Campbell, R.K. Ellis, Nucl. Phys. B Proc. Suppl. **205–206**, 10–15 (2010). https://doi.org/10.1016/j.nuclphysbps.2010.08.011 arXiv:1007.3492 [hep-ph]
37. R. Boughezal, J.M. Campbell, R.K. Ellis, C. Focke, W. Giele, X. Liu, F. Petriello, C. Williams, Eur. Phys. J. C **77**(1), 7 (2017). https://doi.org/10.1140/epjc/s10052-016-4558-y arXiv:1605.08011 [hep-ph]
38. T. Hahn, J. Phys. Conf. Ser. **608**, 012066 (2015). https://doi.org/10.1088/1742-6596/608/1/012066 arXiv:1408.6373 [physics.comp-ph]
39. G. Parisi, R. Petronzio, Nucl. Phys. B **154**, 427–440 (1979). https://doi.org/10.1016/0550-3213(79)90040-3
40. S. Catani and M. Grazzini, Eur. Phys. J. C **72**, 2013 (2012). https://doi.org/10.1140/epjc/s10052-012-2013-2. arXiv:1106.4652 [hep-ph] [erratum: Eur. Phys. J. C **72** (2012), 2132]
41. S. Catani, E. D'Emilio, L. Trentadue, Phys. Lett. B **211**, 335–342 (1988). https://doi.org/10.1016/0370-2693(88)90912-4
42. D. de Florian, M. Grazzini, Phys. Rev. Lett. **85**, 4678–4681 (2000). https://doi.org/10.1103/PhysRevLett.85.4678 arXiv:hep-ph/0008152
43. D. de Florian, M. Grazzini, Nucl. Phys. B **616**, 247–285 (2001). https://doi.org/10.1016/S0550-3213(01)00460-6 arXiv:hep-ph/0108273

44. J. Kuipers, T. Ueda, J.A.M. Vermaseren, J. Vollinga, Comput. Phys. Commun. **184**, 1453–1467 (2013). https://doi.org/10.1016/j.cpc.2012.12.028 arXiv:1203.6543 [cs.SC]

45. J.A.M. Vermaseren, Int. J. Mod. Phys. A **14**, 2037–2076 (1999). https://doi.org/10.1142/S0217751X99001032 arXiv:hep-ph/9806280

46. E. Remiddi, J.A.M. Vermaseren, Int. J. Mod. Phys. A **15**, 725–754 (2000). https://doi.org/10.1142/S0217751X00000367 arXiv:hep-ph/9905237

47. S. Albino, Phys. Lett. B **674**, 41–48 (2009). https://doi.org/10.1016/j.physletb.2009.02.053 arXiv:0902.2148 [hep-ph]

48. A. Vogt, Comput. Phys. Commun. **170**, 65–92 (2005). https://doi.org/10.1016/j.cpc.2005.03.103 arXiv:hep-ph/0408244

49. L. Cieri, C. Oleari, M. Rocco, Eur. Phys. J. C **79**(10), 852 (2019). https://doi.org/10.1140/epjc/s10052-019-7361-8 arXiv:1906.09044 [hep-ph]

50. M.A. Ebert, F.J. Tackmann, JHEP **03**, 158 (2020). https://doi.org/10.1007/JHEP03(2020)158 arXiv:1911.08486 [hep-ph]

51. L. Buonocore, M. Grazzini, F. Tramontano, Eur. Phys. J. C **80**(3), 254 (2020). https://doi.org/10.1140/epjc/s10052-020-7815-z arXiv:1911.10166 [hep-ph]

52. C. Oleari, M. Rocco, Eur. Phys. J. C **81**, 183 (2021). https://doi.org/10.1140/epjc/s10052-021-08878-3 arXiv:2012.10538 [hep-ph]

53. M.A. Ebert, J.K.L. Michel, I.W. Stewart, F.J. Tackmann, JHEP **04**, 102 (2021). https://doi.org/10.1007/JHEP04(2021)102 arXiv:2006.11382 [hep-ph]

54. S. Alekhin, A. Kardos, S. Moch, Z. Trócsányi, Eur. Phys. J. C **81**(7), 573 (2021). https://doi.org/10.1140/epjc/s10052-021-09361-9 arXiv:2104.02400 [hep-ph]

55. L. Buonocore, S. Kallweit, L. Rottoli, M. Wiesemann, arXiv:2111.13661 [hep-ph]

56. S. Catani, M.L. Mangano, P. Nason, L. Trentadue, Nucl. Phys. B **478**, 273–310 (1996). https://doi.org/10.1016/0550-3213(96)00399-9 arXiv:hep-ph/9604351

57. E. Laenen, G.F. Sterman, W. Vogelsang, Phys. Rev. Lett. **84**, 4296–4299 (2000). https://doi.org/10.1103/PhysRevLett.84.4296 arXiv:hep-ph/0002078

58. A. Kulesza, G.F. Sterman, W. Vogelsang, Phys. Rev. D **66**, 014011 (2002). https://doi.org/10.1103/PhysRevD.66.014011 arXiv:hep-ph/0202251

59. J.C. Collins, D.E. Soper, Nucl. Phys. B **197**, 446–476 (1982). https://doi.org/10.1016/0550-3213(82)90453-9

60. J.C. Collins, D.E. Soper, G.F. Sterman, Nucl. Phys. B **250**, 199–224 (1985). https://doi.org/10.1016/0550-3213(85)90479-1

61. R.D. Ball et al. [NNPDF], Eur. Phys. J. C **77**(10), 663 (2017). https://doi.org/10.1140/epjc/s10052-017-5199-5. arXiv:1706.00428 [hep-ph]

62. T. Carli, D. Clements, A. Cooper-Sarkar, C. Gwenlan, G.P. Salam, F. Siegert, P. Starovoitov, M. Sutton, Eur. Phys. J. C **66**, 503–524 (2010). https://doi.org/10.1140/epjc/s10052-010-1255-0 arXiv:0911.2985 [hep-ph]

63. T. Kluge, K. Rabbertz, M. Wobisch, https://doi.org/10.1142/9789812706706_0110. arXiv:hep-ph/0609285